Defects and porosity in zirconia-based nanomaterials

I. Prochazka[1], J. Cizek[1], O. Melikhova[1], F. Lukac[1,2], P. Hruska[1], W. Anwand[3], M.O. Liedke[3], G. Brauer[3], T.E. Konstantinova[4], I.A. Danilenko[4]

[1] *Charles University, Faculty of Mathematics and Physics, Dept. of Low Temperature Physics, Prague, Czech Republic*

[2] *Czech Acad. Sci., Inst. of Plasma Physics, Prague, Czech Republic*

[3] *Helmholtz-Centre Dresden-Rossendorf, Inst. of Radiation Physics, Dresden, Germany*

[4] *Nat. Acad. Sci. of Ukraine, Donetsk Inst. for Physics and Engineering named after O.O. Galkin, Kyiv, Ukraine*

18th ICPA, Aug. 19 – 24, 2018 | Orlando, USA

Talk outline

- Introduction/motivation.
- Experiments.
- Results and discussion.
- Conclusions.
- Acknowledgements.

Introduction / motivation

Zirconia (zirconium dioxide, ZrO_2):

- A wide band gap ($E_g \approx 5 – 7$ eV) semiconductor exhibiting a number of useful thermal, electrical, mechanical and chemical properties,
- A basic constituent of many functional materials.
- Doping with proper metal cations benefits in
  - stabilisation of high temperature tetragonal (*t*-) or cubic (*c*-) phases of zirconia down to room temperature,
  - optimisation of other material characteristics.
- Nanopowders – suitable starting substances for manufacturing sintered ceramics.

There is still continuing interest in investigations of zirconia nanomaterials doped with various metal cations.

Introduction / motivation

Open-volume defects in doped zirconia nanomaterials.

Nanopowders – GBs related defects dominate**.**

- Small open-volume defects:
  - vacancy-like misfit defects situated along GBs ($\tau_V \approx 0.19$ ns),
  - open volumes at intersections of three GBs (triple points, $\tau_t \approx 0.4$ ns).
- Nano- and mesopores – still incomplete knowledge about these structural elements.

Introduction / motivation

Open-volume defects in doped zirconia nanomaterials.

Nanopowders – GBs related defects dominate**.**

- Small open-volume defects:
  - vacancy-like misfit defects situated along GBs ($\tau_V \approx 0.19$ ns),
  - open volumes at intersections of three GBs (triple points, $\tau_t \approx 0.4$ ns).
- Nano- and mesopores – still incomplete knowledge about these structural elements.

Nanoceramics.

- metal cation vacancies inside grains ($\tau_V \approx 0.17$ ns).

Introduction / motivation

Open-volume defects in doped zirconia nanomaterials.

Nanopowders – GBs related defects dominate**.**

- Small open-volume defects:
  - vacancy-like misfit defects situated along GBs ($\tau_V \approx 0.19$ ns),
  - open volumes at intersections of three GBs (triple points, $\tau_t \approx 0.4$ ns).
- Nano- and mesopores – still incomplete knowledge about these structural elements.

Nanoceramics.

- metal cation vacancies inside grains ($\tau_V \approx 0.17$ ns).

Positron annihilation spectroscopy (PAS) – efficient tool of defects investigations into doped zirconia nanopowders and nanoceramics.

Introduction / motivation

Scope of the present talk

- Present talk is focused on zirconia nanopowders and ceramics doped with the MgO and CeO_2 .
- PAS techniques: the conventional positron lifetime (PLT) spectrometry and the variable-energy slow-positron beam spectroscopy were employed.
- Complementary techniques – electron microscopy, mass-density mesurements.

Experiments

Samples

- **ZrO_2 nanopowders** (dopants Mg^{2+}, Ce^{4+}):
  - Initial nanopowders – co-precipitation from water solutions of appropriate salts taken in stoichiometric compositions (developed and performed by Donetsk branch).
  - Calcination @ T_c (1 h in air).
  - Characterisation of nanoparticle size by TEM or XRD (mean particle size between 10 and 20 nm).
  - Compaction of calcined nanopowders into pellets (≈15 mm radius and ≈2 mm thickness) – uniaxial pressure P of 5 kbar.

Experiments

Samples

- **ZrO_2 nanopowders** (dopants Mg^{2+}, Ce^{4+}):
- **Nanoceramics** obtained by sintering compacted ZrO_2 nanopowders @ T_S = 1500 °C (1 h in air).

Experiments

Samples

Basic characteristics of pressure-compacted nanopowders		
Abbrev.; chem. composition (phase [a])	**P [kbar]**	***d* [nm]; T_C / duration**
MgSZ; ZrO_2+10mol.% MgO (T)	5.0	11 nm; 500 °C/1 h
CeSZ; ZrO_2+12mol.% CeO_2 (T)	5.0	9 nm; 500 °C/1 h
[a] T - tetragonal		

Nanopowders of tetragonal ZrO_2 doped with 3 mol.% Y_2O_3 (*t*-YSZ) and 3mol.% Cr_2O_3 , prepared by the similar technique, were involved for comparison.

Experiments

Positron lifetime (PLT) spectroscopy

- A BaF_2 fast–fast delayed-coincidence spectrometer (Becvar et al., 2000).
- Measurements were conducted at room temperature in air.
- Positron/positronium lifetimes up to ≈140 ns were investigated.

Experiments

Slow-positron beam spectroscopy

Magnetically guided positron beam SPONSOR @ HZDR (Anwand et al., 1995, 2012):

- range of positron energies E from 0.03 to 35 keV,
- single HPGe detector measurements (1.05 keV FWHM, 5×10^5 counts in 511 keV peak),
- shape parameters, $S(E)$ and $W(E)$,
- relative positronium 3γ-fractions, $F_{3\gamma}(E)$.

Results & discussion

PLT spectroscopy

Ortho-Ps data on pressure-compacted nanopowders (lifetimes $\tau_{oPs,i}$, pore radii R_i and rel. intensities I_{Ps})

Sample	$\tau_{oPs,1}$ [ns]	R_1 [nm] [a)]	$\tau_{oPs,2}$ [ns]	R_2 [nm] [a)]	I_{Ps} [%]
t-YSZ	7.8 (11)	0.61 (4)	70.7 (22)	6.1 (9)	21.4 (6)
MgSZ	5.6 (6)	0.52 (3)	64.9 (14)	4.4 (3)	17.4 (19)
CeSZ	6.4 (4)	0.55 (2)			0.6 (2)

[a)] Pore radii estimated from Wada & Hyodo model, corrected for ortho-para conversion in air.

Results & discussion

PLT spectroscopy

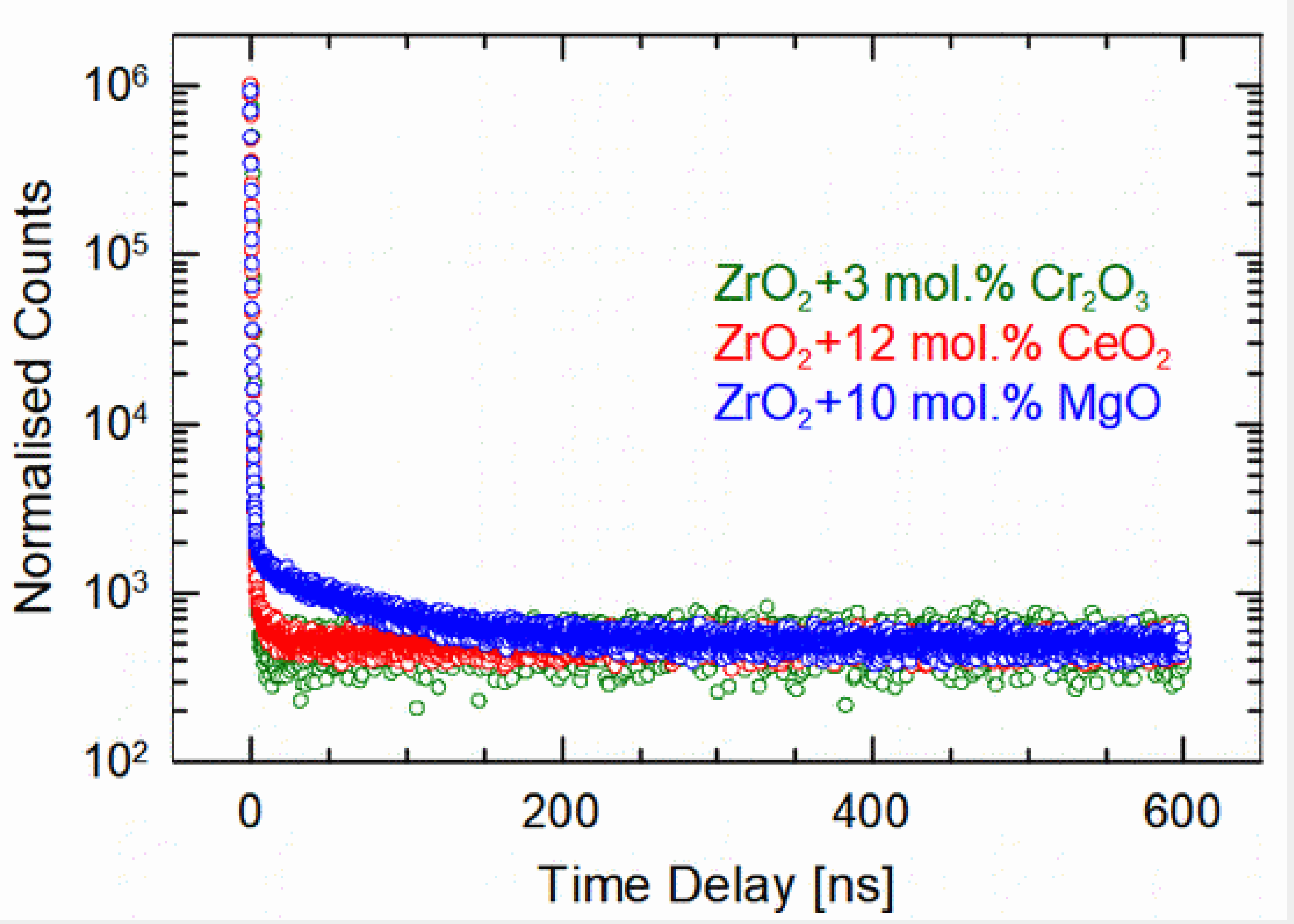

Results & discussion

PLT spectroscopy

Ortho-Ps data on pressure-compacted nanopowders (lifetimes $\tau_{oPs,i}$, pore radii R_i and rel. intensities I_{Ps})

Sample	$\tau_{oPs,1}$ [ns]	R_1 [nm] [a)]	$\tau_{oPs,2}$ [ns]	R_2 [nm] [a)]	I_{Ps} [%]
t-YSZ	7.8 (11)	0.61 (4)	70.7 (22)	6.1 (9)	21.4 (6)
MgSZ	5.6 (6)	0.52 (3)	64.9 (14)	4.4 (3)	17.4 (19)
CeSZ	6.4 (4)	0.55 (2)			0.6 (2)

[a)] Pore radii estimated from Wada & Hyodo model, corrected for ortho-para conversion in air.

In *t*-YSZ and MgSZ, two ortho-Ps components observed:

- the larger pores (R_2≈5 nm),
- the smaller pores (R_1≈0.6 nm).

Results & discussion

PLT spectroscopy

Ortho-Ps data on pressure-compacted nanopowders (lifetimes $\tau_{oPs,i}$, pore radii R_i and rel. intensities I_{Ps})					
Sample	**$\tau_{oPs,1}$ [ns]**	**R_1 [nm] [a)]**	**$\tau_{oPs,2}$ [ns]**	**R_2 [nm] [a)]**	**I_{Ps} [%]**
t-YSZ	7.8 (11)	0.61 (4)	70.7 (22)	6.1 (9)	21.4 (6)
MgSZ	5.6 (6)	0.52 (3)	64.9 (14)	4.4 (3)	17.4 (19)
CeSZ	6.4 (4)	0.55 (2)			0.6 (2)

[a)] Pore radii estimated from Wada & Hyodo model, corrected for ortho-para conversion in air.

In CeSZ, only shorter oPs component could be revealed:

- the smaller pores ($R_1 \approx 0.6$ nm) are evidenced.

Results & discussion

PLT spectroscopy

- In zirconia-based nanopowders doped with several other metal cations (monoclinic ZrO_2, cubic YSZ, ZrO_2 doped with Eu^{3+}, Gd^{3+}, Lu^{3+}.), similar two-component pattern like the *t*-YSZ and MgSZ case were observed, too:
  - $\tau_{oPs,1} \approx 7.5$ ns, $I_{p.o.,1} \approx 0.7$ %, $R_1 \approx 0.6$ nm;
  - $\tau_{oPs,2} \approx 70$ ns, $I_{p.o.,2} \approx 7.5$ %, $R_2 \approx 4.5$ to 8.5 nm, originated likely from cavities between primary nanoparticle aggregates.

Results & discussion

PLT spectroscopy

- In zirconia-based nanopowders doped with several other metal cations (monoclinic ZrO_2, cubic YSZ, ZrO_2 doped with Eu^{3+}, Gd^{3+}, Lu^{3+}.), similar two-component pattern like the *t*-YSZ and MgSZ case were observed, too:
  - $\tau_{oPs,1} \approx 7.5$ ns, $I_{p.o.,1} \approx 0.7$ %, $R_1 \approx 0.6$ nm;
  - $\tau_{oPs,2} \approx 70$ ns, $I_{p.o.,2} \approx 7.5$ %, $R_2 \approx 4.5$ to 8.5 nm, originated likely from cavities between <u>primary nanoparticle aggregates</u>.

Aggregation of primary nanoparticles (Ito et al., 1999):

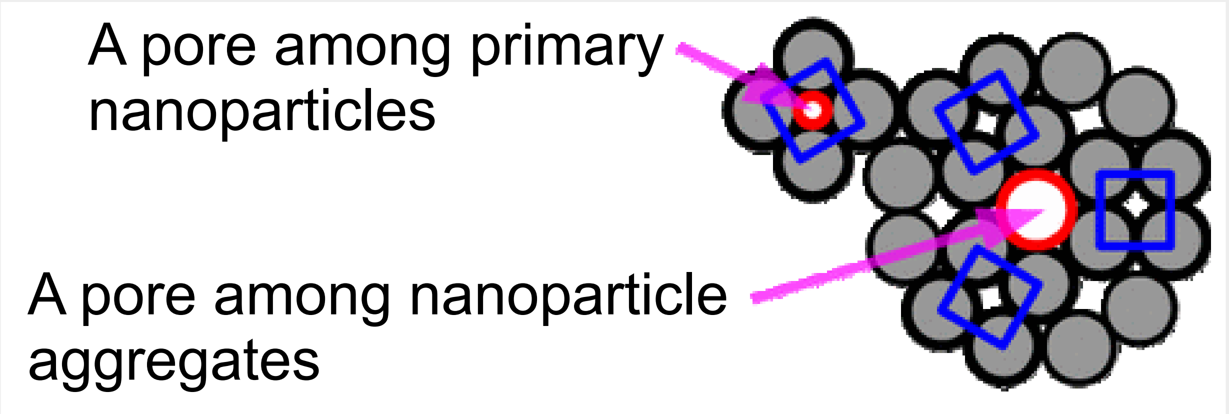

Results & discussion

PLT spectroscopy

- In zirconia-based nanopowders doped with several other metal cations (monoclinic ZrO_2, cubic YSZ, ZrO_2 doped with Eu^{3+}, Gd^{3+}, Lu^{3+}.), similar two-component pattern like the *t*-YSZ and MgSZ case were observed, too:
  - $\tau_{oPs,1} \approx 7.5$ ns, $I_{p.o.,1} \approx 0.7$ %, $R_1 \approx 0.6$ nm;
  - $\tau_{oPs,2} \approx 70$ ns, $I_{p.o.,2} \approx 7.5$ %, $R_2 \approx 4.5$ to 8.5 nm, originated likely from cavities between primary nanoparticle aggregates.

Aggregation of primary nanoparticles (Ito et al., 1999):

Aggregates of 14 particles reported in YSZ.

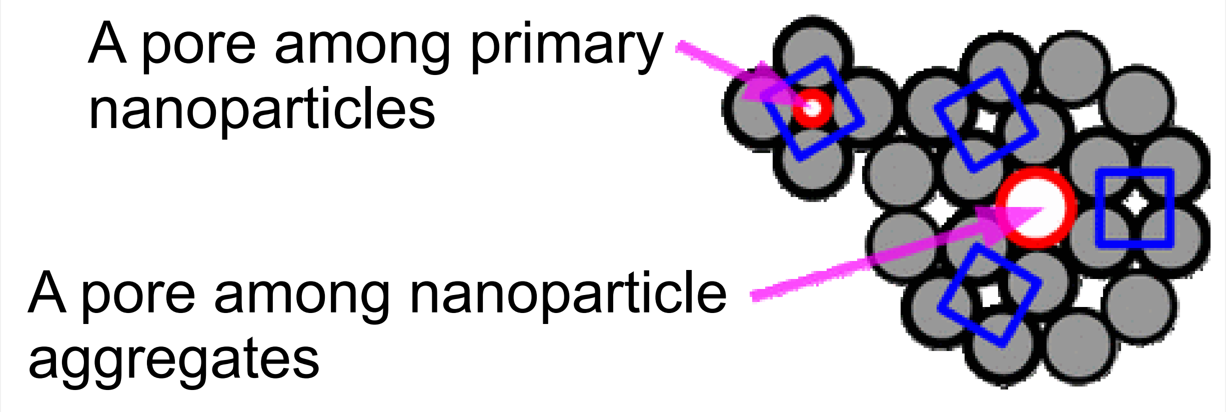

Results & discussion

PLT spectroscopy

- In zirconia-based nanopowders doped with several other metal cations (monoclinic ZrO_2, cubic YSZ, ZrO_2 doped with Eu^{3+}, Gd^{3+}, Lu^{3+}.), similar two-component pattern like the *t*-YSZ and MgSZ case were observed, too:
  - $\tau_{\mathrm{oPs},1} \approx 7.5$ ns, $I_{\mathrm{p.o.},1} \approx 0.7$ %, $R_1 \approx 0.6$ nm;
  - $\tau_{\mathrm{oPs},2} \approx 70$ ns, $I_{\mathrm{p.o.},2} \approx 7.5$ %, $R_2 \approx 4.5$ to 8.5 nm, originated likely from cavities between <u>primary nanoparticle aggregates</u>.

Aggregates – equal-sized rigid spherical particles:

Packing factor ξ : $\xi = 0.75$ – dense packing,
$\xi = 0.64$ – random close packing,
$\xi \approx 0.55$ – random loose packing.

Results & discussion

PLT spectroscopy

- In zirconia-based nanopowders doped with several other metal cations (monoclinic ZrO_2, cubic YSZ, ZrO_2 doped with Eu^{3+}, Gd^{3+}, Lu^{3+}.), similar two-component pattern like the *t*-YSZ and MgSZ case were observed, too:
  - $\tau_{oPs,1} \approx 7.5$ ns, $I_{p.o.,1} \approx 0.7$ %, $R_1 \approx 0.6$ nm;
  - $\tau_{oPs,2} \approx 70$ ns, $I_{p.o.,2} \approx 7.5$ %, $R_2 \approx 4.5$ to 8.5 nm, originated likely from cavities between primary nanoparticle aggregates.

Aggregates – equal-sized rigid spherical particles:

$L = 4\ R_{oPs,2} / 3$ – the mean free path in a hole,

then number of particles forming an aggregate is ≈ 7.

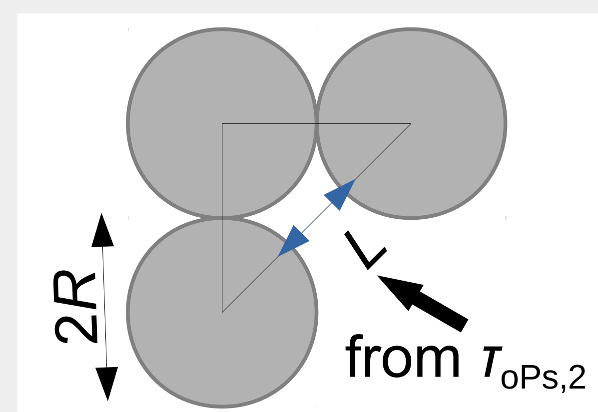

Results & discussion

PLT spectroscopy

- In zirconia-based nanopowders doped with several other metal cations (monoclinic ZrO_2, cubic YSZ, ZrO_2 doped with Eu^{3+}, Gd^{3+}, Lu^{3+}.), similar two-component pattern like the *t*-YSZ and MgSZ case were observed, too:
  - $\tau_{oPs,1}$ ≈ 7.5 ns, $I_{p.o.,1}$ ≈ 0.7 %, R_1 ≈ 0.6 nm;
  - $\tau_{oPs,2}$ ≈ 70 ns, $I_{p.o.,2}$ ≈ 7.5 %, R_2 ≈ 4.5 to 8.5 nm, originated likely from cavities between primary nanoparticle aggregates.

Aggregates – equal-sized rigid spherical particles:

However:

? terms 'equal-sized', 'rigid' or 'spherical',
? randomness of packing.

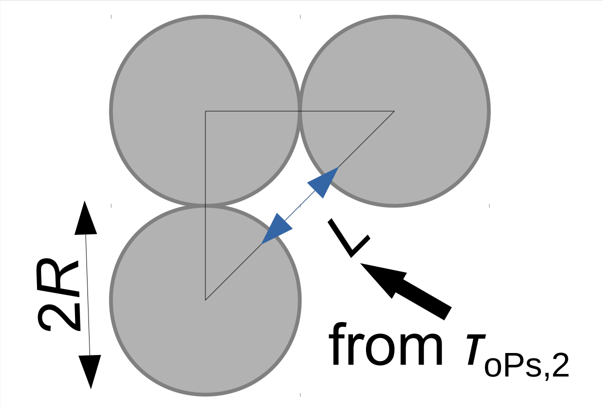

Results & discussion

PLT spectroscopy

- In zirconia-based nanopowders doped with several other metal cations (monoclinic ZrO_2, cubic YSZ, ZrO_2 doped with Eu^{3+}, Gd^{3+}, Lu^{3+}.), similar two-component pattern like the *t*-YSZ and MgSZ case were observed, too:
  - $\tau_{oPs,1} \approx 7.5$ ns, $I_{p.o.,1} \approx 0.7$ %, $R_1 \approx 0.6$ nm;
  - $\tau_{oPs,2} \approx 70$ ns, $I_{p.o.,2} \approx 7.5$ %, $R_2 \approx 4.5$ to 8.5 nm, originated likely from cavities between primary nanoparticle aggregates.
- CeSZ case is an exclusion:
  - the larger pores likely do not occur (aggregation of primary nanoparticles does not take place ?).

Results & discussion

Measured mass densities

Mass density data on pressure-compacted nanopowders		
Sample	**ρ [g/cm^3]**	**ρ/ρ_{th} [a)]**
t-YSZ	2.922 (5)	0.478
MgSZ	2.25 (15)	0.37
CeSZ	2.750 (3)	0.450
[a)] ρ_{th} = 6.11 g/cm^3 adopted.		

MgSZ, *t*-YSZ ceramics: $\rho \approx 5.8$ g/cm^{-3} (≈ 95 % of ρ_{th}).

Pressure-compacted nanopowders – random close- (or loose)-packed aggregates of dense packed nanoparticles.

Results & discussion

Further evidence for absence of the large pores in CeSZ (contrary to MgSZ and YSZ, RESZ):

- electron microscopy,
- slow-positron beam spectroscopy.

Results & discussion

TEM observation on nanopowders

MgSZ

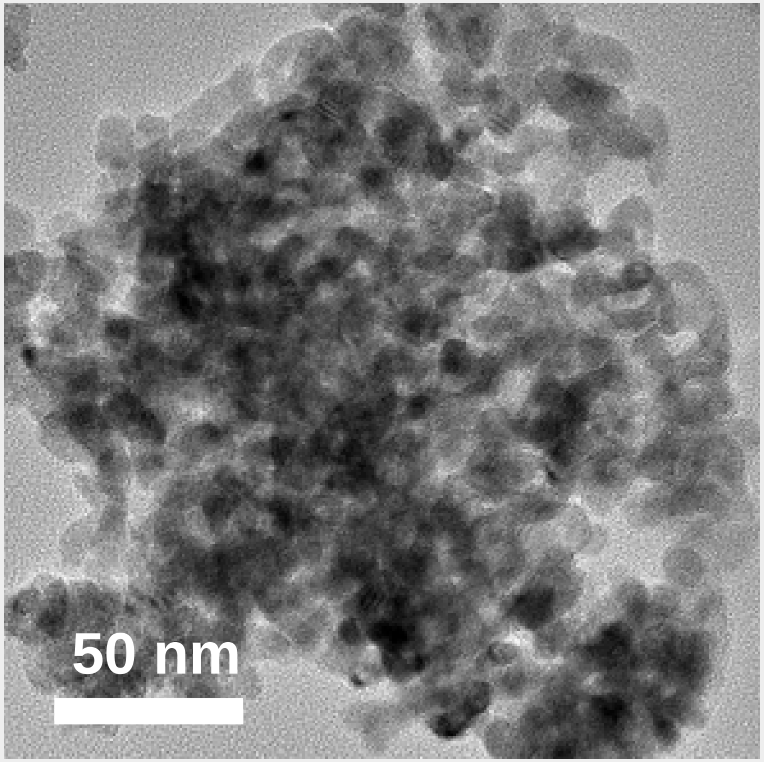

CeSZ

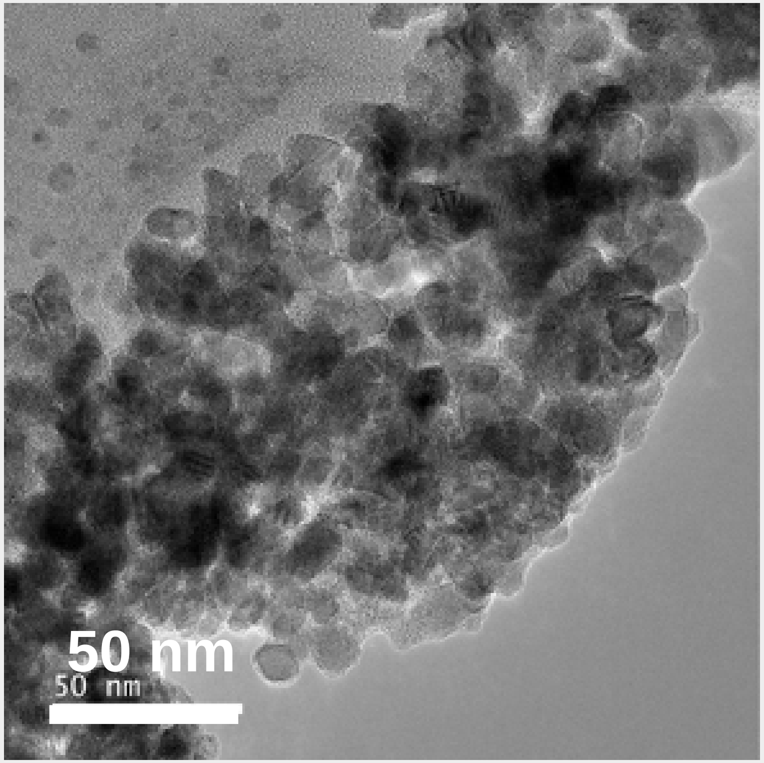

Aggregates of primary nanoparticles: more visible in MgSZ than in CeSZ.

Results & discussion

TEM observation on nanopowders

MgSZ

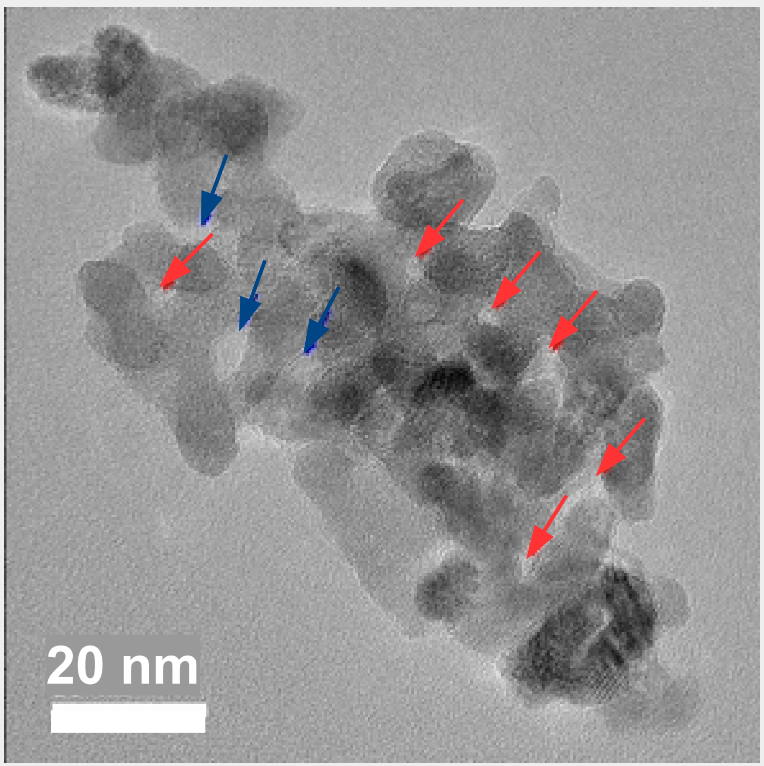

CeSZ

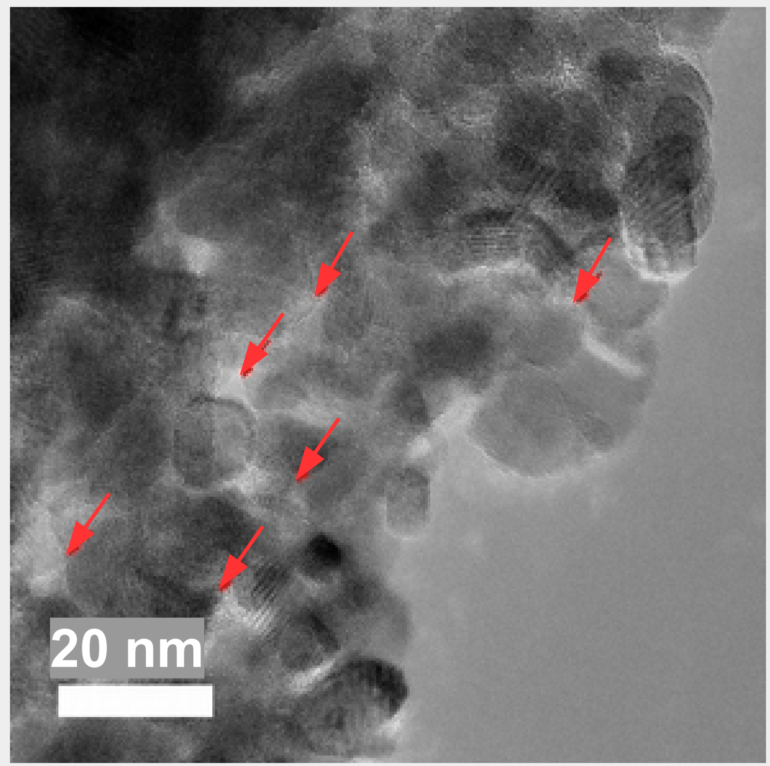

smaller pores (1 to 2 nm);

larger pores (4 to 5 nm, seen in MgSZ, not in CeSZ).

Larger pores: more visible in MgSZ than in CeSZ. Pore sizes: reasonable consistency with PLT data.

Results & discussion

Slow-positron beam spectroscopy

Vanishing of $F_{3\gamma}$ in the bulk – the strongest evidence of an absence of large pores in CeSZ:

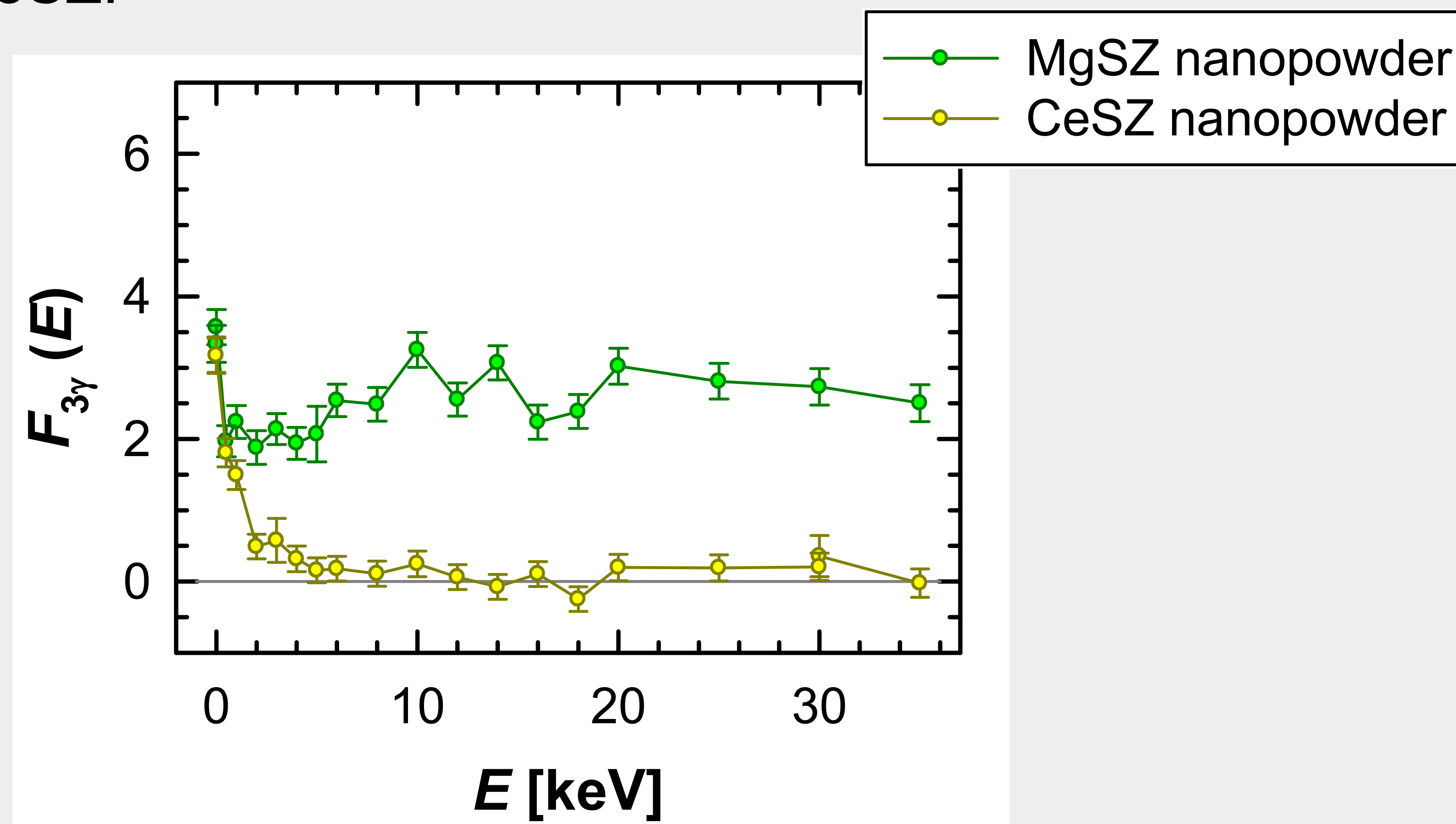

Results & discussion

Slow-positron beam spectroscopy

Vanishing of $F_{3\gamma}$ in the bulk – the strongest evidence of an absence of large pores in CeSZ:

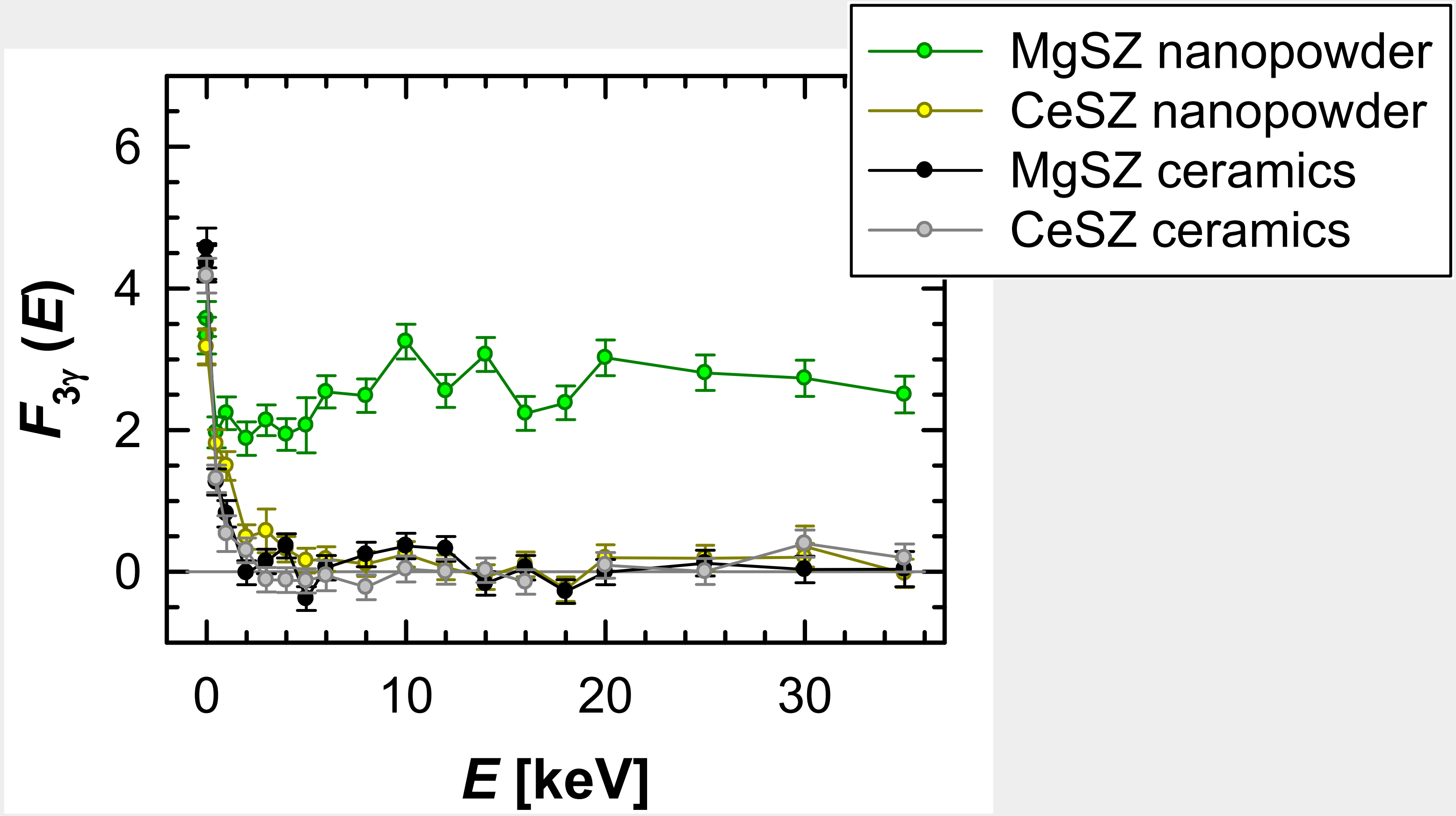

Conclusions

- In zirconia nanopowders doped with yttria, magnesia, two kinds of pores with radii estimated as R_1≈0.6 nm and R_2≈4.5 to 8.5 nm.
- The larger pores are likely cavities between small nanoparticle aggregates (tentatively ≈7 primary nanoparticles).
- **The ZrO_2+CeO_2** seems to contain the *smaller pores* only, but not the large ones, pointing toward an absence of significant particle aggregation. This system thus may receive some attraction for applications when particle aggregation is unwanted.

Acknowledgements

- **ICPA-18 Organisers:** hospitality and providing a possibility to present results at this Conference.
- **Finance funding:** Czech Science Foundation (project P108/12/G043), Nat. Acad. Sci. of Ukraine (project 89/12-H).
- **The four Institutions:** supporting members of teams in fruitful co-operation on working-out this Contribution.

Thank you
for kind listening !

Swan song

Backup

Relative positronium (Ps) 3γ-fractions, $F_{3\gamma}(E)$

$$F_{3\gamma}(E) = R(E) - R_{ref} \quad ,$$

where

$$R(E) \equiv \frac{V(E)}{A_{2\gamma}(E)} \quad ,$$

$$R_{ref} \equiv \frac{V_{ref}}{A_{2\gamma,ref}} \quad .$$

'*ref*' state – bulk reference material with no Ps formation, measured with the same setup,

$A_{2\gamma}(E), A_{2\gamma,ref}$ – 511 keV peak areas,

$V(E)$, V_{ref} – background subtracted areas left to 511 keV peak (480 – 500 keV region).

Backup

Schematic view of packing of rigid spherical particles

Particle

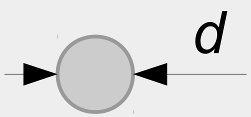

$$V_p = \frac{\pi}{6} d^3$$

Particle aggregate

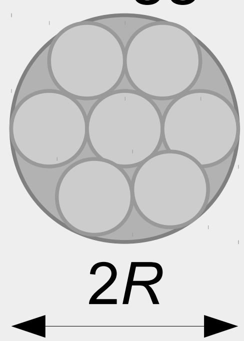

$$V_{ag} = \frac{4\pi}{3} R^3$$

Packing of aggregates

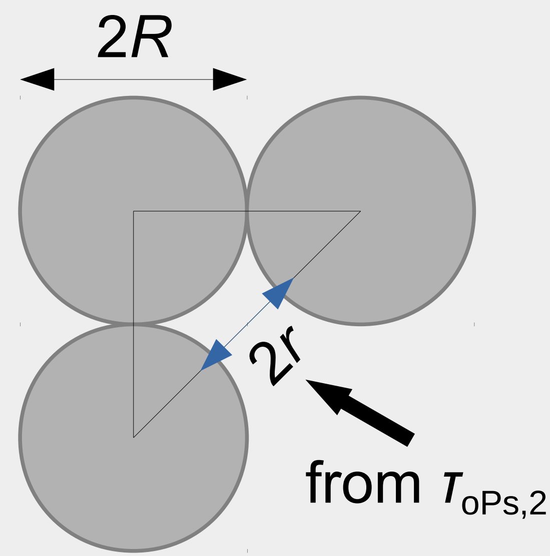

$$2r \approx 2R \cdot \left(\sqrt{2} - 1\right)$$

Packing factor ξ :

- ξ = 0.75 – dense packing,
- ξ = 0.64 – random close packing,
- $\xi \approx$ 0.55 – random loose packing.

$$N_p = \xi \cdot V_{ag} / V_p$$